

# The Effect of Particle Size in Second Harmonic Generation from the Surface of Spherical Colloidal Particles. I: Experimental Observations<sup>†</sup>

Shih-Hui Jen,<sup>‡,⊥</sup> Grazia Gonella,<sup>§</sup> and Hai-Lung Dai<sup>\*,§</sup>

Department of Chemistry, University of Pennsylvania, Philadelphia, Pennsylvania 19104, and Department of Chemistry, Temple University, Philadelphia, Pennsylvania 19122

Received: February 3, 2009; Revised Manuscript Received: February 25, 2009

The size of the colloidal particle has a dramatic effect on the efficiency of optical second harmonic generation (SHG) from the particle surface. This effect is illustrated with the second harmonic intensity measured from submicrometer polystyrene beads adsorbed with malachite green dye molecules in aqueous solution, both in the forward direction and as a function of the scattering angle in the horizontal plane. In the forward scattering direction, the SHG efficiency initially increases rapidly with the particle size. The efficiency peaks at  $\sim 1 \mu\text{m}$  diameter and then decreases with the particle size. The majority of the SH light generated from the particle surface scatters away from the forward direction for smaller particles. In particular for particles with diameter smaller than 100 nm the position of the maximum is nearly  $90^\circ$  away from the forward direction. A straightforward phenomenological model is used to predict that the angle of maximum SH efficiency tilts more toward the forward direction for particles with larger diameter as well as higher refractive index.

## I. Introduction

In colloids, interactions between the colloidal particle and the solvent as well as interparticle interactions have direct impact on the dispersion stability of the colloidal system. These interactions depend on the properties of the colloidal particle surface which can be altered through adsorption and surface treatment. Understanding the influence of surface characteristics on colloidal properties requires experimental capabilities for determining the structure and kinetic/dynamic processes at colloidal particle surfaces.<sup>1,2</sup>

The nonlinear optical phenomenon, second harmonic generation (SHG), is forbidden in the dipole approximation in the bulk of a centrosymmetric sphere but is allowed at the surface of such a particle because here the inversion symmetry is broken. Unfortunately, for particles made of materials with relatively low hyper-polarizability such as polystyrene beads, the SHG from the particle surface is too small to be detected. On the other hand, when molecules possessing second-order polarizabilities adsorb onto the particle surface, SHG may be detectable. In this case, SHG arises only from molecules adsorbed at the surface but not from the ones dissolved in the solution. The solvated molecules are randomly oriented and thus would not facilitate SHG, while the surface-adsorbed molecules with orientation order would give nonzero susceptibility.

SHG from the surface-adsorbed molecules in colloids has been developed as an effective tool for *in situ* probing of the adsorption density, free energy,<sup>3–6</sup> surface potential,<sup>7</sup> and structure<sup>8</sup> for a variety of molecules such as dyes,<sup>8–11</sup> surfactants,<sup>4</sup> and biopolymers<sup>5</sup> on a wide range of colloidal particles such as polystyrene beads,<sup>3–5,8–11</sup> clay,<sup>12</sup> and semiconductor

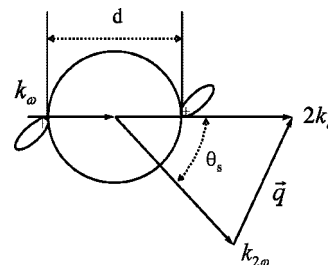


**Figure 1.** Schematic illustration of the phase matching condition for the SH field generated from molecules adsorbed at the surface of a spherical particle with diameter  $d$ . The SH wave vector,  $k_{2\omega}$ , defines the scattering angle  $\theta_s$ , from the fundamental wave vector,  $k_\omega$ .

particles.<sup>13</sup> It can even be used for monitoring kinetic transport through the membrane of liposome vesicles.<sup>14,15</sup>

In the use of SHG to probe colloidal particle surfaces, an obvious concern is the particle size. Intuitively, molecules adsorbed on the opposite sides of the spherical particle with a size much smaller than the optical coherence length may cancel each other and render SHG nondetectable. Because of this concern the earlier studies have been on micrometer- or submicrometer-sized particles. Only very recently, SHG detection of molecular adsorption on polystyrene particles with diameter as small as 50 nm has been reported.<sup>16</sup> In order to evaluate the utility of SHG for characterizing colloidal particles and to understand the significance of the measured SHG intensity, the effect of particle size needs to be understood. In the very first report of SHG from the surface of centrosymmetric particles in a liquid solution, Eisenthal and co-workers presented a simple, yet illustrative, model to explain how a centrosymmetric object can give SHG.<sup>10</sup> In this model for two identical molecules adsorbed on opposite sides, with opposite orientations and separated by the particle diameter  $d$  (Figure 1), it is shown that if  $d$  is comparable to or larger than the incident wavelength  $\lambda_\omega$ , the second-order molecular polarizations of the two molecules would not cancel each other. However, when  $d$  is much smaller than  $\lambda_\omega$ , the second harmonic field is zero. While this model is

<sup>†</sup> Part of the “George C. Schatz Festschrift”.

\* To whom all correspondence should be addressed. E-mail: hldai@temple.edu.

<sup>‡</sup> University of Pennsylvania.

<sup>§</sup> Temple University.

<sup>⊥</sup> Present address: Department of Chemistry, University of Colorado, Boulder, CO.

practically useful for evaluating the SH signal generated along the fundamental beam propagation direction (the forward direction), we will show that it can be modified for predicting SHG at large scattering angles which arises from the interference of all SH fields generated from molecules adsorbed over the entire particle surface. The shape of the SH intensity scattering pattern, which results from the interference of all the SH waves generated by the entire surface sources, depends on the size and the refractive index of the particle, in addition to the light wavelengths. For instance, different patterns of SH light scattering have been observed for particles with different sizes.<sup>8,10</sup>

To understand how the SH signal scatters in all solid angles, not just the forward direction, a more precise characterization, both theoretically and experimentally, is needed. In this paper, we report the SH intensity measured in the forward direction as well as at all scattering angles as a function of the particle size. It will be shown that for the malachite green dye adsorbed on polystyrene spherical particles in water, the maximum of the SH intensity moves away from the forward direction. The experimental observations, including the angular distribution pattern of the SH intensity for the various particle sizes, can be quantitatively accounted for by the nonlinear Rayleigh–Gans–Debye model. The details of this theoretical model as well as its limits in terms of the particle size and refractive indexes of the particle and the solution will be presented as Part II of this report.

## II. Experimental Section

The source for the fundamental light is a Ti:sapphire laser (Coherent Mira Seed) pumped by an Ar ion laser (Coherent Innova 310) which provides nominally 50-fs long pulses at 840 nm with less than 5 nJ pulse energy at a 76 MHz repetition rate. The femtosecond laser pulses are used because they provide the high peak power necessary for the nonlinear optical process, while their low pulse energy causes no heating or photochemical effects from light absorption in the sample. The s-/p-polarized (perpendicular/parallel to the scattering plane) fundamental light is focused by a 5-cm focal length lens into a  $\sim 50$   $\mu\text{m}$  beam waist inside the colloidal sample. At the focus the peak intensity of the light is approximately  $4 \times 10^9$  W/cm<sup>2</sup>.

SHG from the sample can be measured in the forward scattering direction, i.e. the same direction as the fundamental, or at other scattering angles in the horizontal plane. In the forward direction ( $\theta = 0^\circ$ ), the laser beam collected by a 5-cm focal lens and collimated by a 8-in. – 4-in. lens assembly, after exiting the sample, passes through a set of band-pass filters (Schott BG 39) and a monochromator (2 nm bandwidth). The rectangular monochromator slit restricts light collection to within  $\pm 20^\circ$  in the plane perpendicular to the scattering plane and  $\pm 2^\circ$  in the scattering plane. The SH signal is then detected by a photomultiplier (Hamamatsu R585), amplified and processed through a correlated photon counting system that suppresses statistical random noise with a discrimination voltage of  $-100$  mV when the photomultiplier tube (PMT) is powered at  $-1300$  V. The signal collected is averaged over 1 s.

In the experimental setup<sup>9</sup> in which the SH intensity is detected as a function of the scattering angle  $\theta_s$ , the scattered light is collected from the laser beam–sample intersection region by a 3-in. focal length lens, passed through a Glan-Taylor prism polarizer (Karl Lambrecht, extinction ratio  $<0.0005$ ) for polarization selection, and a band-pass filter for filtering out the fundamental, and collimated by a collimator (Thorlabs, F230SMA-A) into an optical fiber (numerical aperture, NA:

0.22). The light exiting the fiber is then focused by a 4-in. focal length lens and passes through the filters for detection by the PMT. The detection angle resolution is set by an iris, placed in front of the 3-in. lens, with an aperture angle of  $5^\circ$  or  $2^\circ$  for 0.2 or 0.99  $\mu\text{m}$  diameter particles, respectively. The iris, collimation lens, polarizer, band-pass filter, and the entrance end of fiber are mounted on an arm of a rotating stage set on the optical table. The center of the rotator is set at the focal point of the fundamental beam. Angle-resolved SHG (ARSHG) has been performed with s-in/p-out and p-in/p-out configurations at scattering angle  $\theta_s$  measured clockwise, from  $-90^\circ$  to  $120^\circ$ .

For the titration experiments in which the concentration of the malachite green (MG) dye is changed, the sample is a liquid jet produced by a flow system. The colloidal solution is stored in a reservoir that is constantly stirred with a magnetic stirrer and circulated by a liquid pump through a pressed stainless steel nozzle (inner diameter 1/16 in.) to form the liquid jet. Using the jet avoids any window effects from a sample holder, including dye-molecule burning and SHG generated at the window surfaces. The flow system allows titration of the dye into the colloid solution. The MG dye, in a known high concentration in the same solvent as that for the colloid, is added into the reservoir through a digital titration burette. For the ARSHG measurements, a cylindrical cell (6 mm outer and 3 mm inner diameter in glass) is used to contain the colloidal sample. The sample cell is mounted on a two-dimensional translational stage for position adjustment. The focal point of the fundamental beam is roughly located at the center of the sample cell. Here the colloidal solution in the cell is prepared at a MG concentration so that the polystyrene (PS) particle surface is saturated with MG molecules. The signal detected at twice the frequency of the fundamental may arise from two-photon fluorescence from the MG dye in the solution in addition to the surface-adsorbed MG molecules. The former can be measured from a solution without the PS particle but with the same MG concentration and subtracted from the total signal to result in the SH signal. This process also eliminates all window-generated SHG in the signal.

In the angle-resolved experiments, the colloids consist of PS spherical particles with charge-neutral surface (no surface termination) (Interfacial Dynamics Corporation). These particles are hereafter designated as the PPS particles. In the forward efficiency experiments, the PS particles with negatively charged surface (sulfate  $-\text{SO}_3^-$  termination) (Polyscience) are used. They are designated as the PSS particles. All colloids are in aqueous solution. All particles are spherical with uniform diameter (variation of diameters ranges from 2.0 to 5.9%). In each experiment, a small amount of the stock solution is diluted up to a total volume of 250 mL with its pH adjusted to 4.1 by adding 0.01 N HCl aqueous solution. Malachite green exists in the cationic form at pH 4.1.

## III. Results and Discussion

In order to examine the effect of particle size in SHG from colloidal particle surfaces, we measure the SH intensity from particles of different sizes. We assume that the adsorption configuration is identical for all PS particles independently from the particle size. The surface curvature effect has been found to be important in considering molecules such as alkanethiols adsorbed on gold nanoparticles with sizes smaller than 20 nm.<sup>17</sup> This consideration is disregarded since the area the MG molecule occupies is much less than 1 nm<sup>2</sup> so even for the smallest particle (diameter  $\sim 50$  nm) the local surface can be considered to be planar. The surface adsorption density,

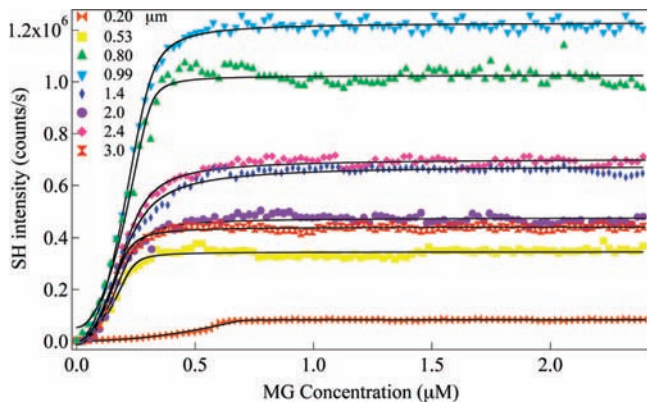


**Figure 2.** SH adsorption isotherms of MG on the surface of PSS particles with diameters, from bottom up, as 0.20, 0.53, 3.0, 2.0, 1.4, 2.4, 0.80, and 0.99  $\mu\text{m}$ . The isotherms are measured as the SH intensity in the forward direction as a function of the MG concentration in the solution. The solid lines are nonlinear least-squares fittings using the modified Langmuir model.

**TABLE 1: Density of MG Molecules Adsorbed on the Surface of PSS Particles As Obtained from the Fit of the SHG Adsorption Isotherms<sup>a</sup>**

diameter ( $\mu\text{m}$ )	density of sulfate group (in number of $-\text{SO}_3^-/\mu\text{m}^2$ )	maximum adsorption density (in number of $\text{MG}/\mu\text{m}^2$ )
0.20	$3.98 \times 10^4$	$1.21 (\pm 0.06) \times 10^5$
0.53	$2.38 \times 10^5$	$2.18 (\pm 0.32) \times 10^5$
0.81	$3.25 \times 10^5$	$2.88 (\pm 0.08) \times 10^5$
0.99	$2.47 \times 10^5$	$3.17 (\pm 0.15) \times 10^5$
1.4	$3.08 \times 10^5$	$3.57 (\pm 0.16) \times 10^5$
2.0	$4.38 \times 10^5$	$4.92 (\pm 0.32) \times 10^5$
2.4	$5.03 \times 10^5$	$4.61 (\pm 0.21) \times 10^5$
3.0	$2.23 \times 10^5$	$5.35 (\pm 0.28) \times 10^5$

<sup>a</sup> The densities of the sulfate functional groups on the surface of the particles provided by the supplier are listed as well.

however, may be different since particles with different sizes are synthesized using different methods, and the density of surface functional groups may be different. For this reason, we first measure the adsorption density of MG on PSS particles in a wide range of sizes. The measured intensity will then be normalized with respect to the density of the adsorbed MG molecules as well as the particle concentration.

**A. Adsorption Density of MG on PSS.** The saturation surface coverage (the maximum adsorption density) of MG on the PSS particles can be obtained from a Langmuir adsorption model analysis of the adsorption isotherm. Figure 2 shows the adsorption isotherms of MG on eight PSS particle sizes ranging from 0.2 to 3.0  $\mu\text{m}$  in diameter, measured as the SH intensity as a function of the MG concentration in the solution. These isotherms can be analyzed through nonlinear least-squares fitting using the modified Langmuir model.<sup>3,4</sup> The maximum surface density obtained from the fitting as well as the density of the surface sulfate group reported from the commercial supplier for the PSS particles with a variety of sizes are listed in Table 1.

**B. Particle Size Effect in SHG in the Forward Direction.** Once the density of adsorbed molecules on the particle surface is known, SHG efficiency, defined as the amount of the SH intensity generated per surface-adsorbed dye molecule, from different sized particles can be compared. The measured SH intensity from a colloidal system can be related to the particle surface area  $a$ , the colloidal particle number density  $n$ , the density  $N_s$  of the adsorbed molecules with orientation-averaged molecular polarizability  $\langle\beta^{(2)}\rangle$ , and the fundamental light intensity  $I_\omega$  as:<sup>10,18–20</sup>

$$I_{2\omega} \propto anN_s^2\langle\beta^{(2)}\rangle^2I_\omega^2 \quad (1)$$

The SH efficiency that varies with particle size is the proportional constant in eq 1 and can be obtained as:

$$\text{SH efficiency} \propto \frac{I_{2\omega}}{anN_s^2\langle\beta^{(2)}\rangle^2I_\omega^2} \quad (2)$$

Another factor related to the particle size that we need to consider in experimentally evaluating the SH efficiency from the measured SH intensity is the loss of the fundamental and the SH light intensity due to Rayleigh scattering off the different sized colloidal particles in the beam path. For example, as calculated from the linear Mie scattering theory<sup>21–23</sup> the 1- $\mu\text{m}$  diameter PSS particle would have a linear scattering coefficient at the fundamental,  $Q_F$ , and SH wavelengths,  $Q_{SH}$ , of 3.58 and 1.55 respectively. This scattering loss can be accounted for by a scattering coefficient  $C_i$  which is evaluated as:

$$C_i = \sum_i \left( \exp\left(Q_{SH}nL_{SH}^i \frac{\pi D^2}{4}\right) \exp\left(-2Q_F nL_F^i \frac{\pi D^2}{4}\right) \right) \quad (3)$$

where  $L_F^i$  is the length that the fundamental light trespasses in the sample before reaching the  $i$ th particle and  $L_F^{SH}$  is the length the SH light traverses in the sample after the  $i$ th particle. Note the factor of 2 in the exponent associated with the fundamental because the SH intensity generated is proportional to the square of the fundamental intensity. We evaluate this effect for each particle size through a numerical model. The 1-mm thick jet is divided into 11 portions ( $i = 1-11$ ), and the coefficients of each of the regions are calculated for the distance at the center of the region. As a result, for example, for the 1- $\mu\text{m}$  diameter PSS particles,  $C_i$  is calculated as 0.63. Finally, the SH intensity measured is normalized by this coefficient to produce the SH intensity for comparison:  $I_{2\omega} = I_{2\omega}(\text{expt})/C_i$ .

After being normalized by the fundamental power, the particles concentration, the number of MG molecules adsorbed on the surface, and the area, the experimentally measured SH intensity in the forward scattering direction as a function of particle size is shown in Figure 3 before (blue) and after (red) the multiple scattering correction. It appears that the 0.99- $\mu\text{m}$  diameter PSS is most efficient in generating the SH signal in the forward direction. As the particle diameter increases from 1  $\mu\text{m}$ , SH efficiency decreases slowly: SH efficiency of the 2- $\mu\text{m}$  PSS is about half of that of the 1- $\mu\text{m}$  PSS, and for the 3- $\mu\text{m}$  PSS it is about a quarter. On the other hand, when the particle diameter decreases from 1  $\mu\text{m}$ , SH efficiency drops very quickly: Comparing with the 1- $\mu\text{m}$  PSS, the efficiency of the 0.2- $\mu\text{m}$  PSS has decreased to less than 10%. In the forward direction, SHG from polystyrene particles smaller than 0.1  $\mu\text{m}$  and is hardly detectable.

**C. SHG from Smaller Particles at Large Scattering Angles.** The maximum SH intensity, as a function of scattering angle, tilts toward larger scattering angles with decreasing particle size. This trend can be clearly noted in Figure 4 in which the angular distribution of the SH light from 1-, 0.20-, and 0.05- $\mu\text{m}$  PPS particles detected with p-in/p-out and s-in/p-out polarization configuration is shown. The maximum SH intensity from 1- $\mu\text{m}$  PPS particles occurs at around  $10^\circ$ , while the most intense SH light from 0.05  $\mu\text{m}$  is detected around  $90^\circ$ .

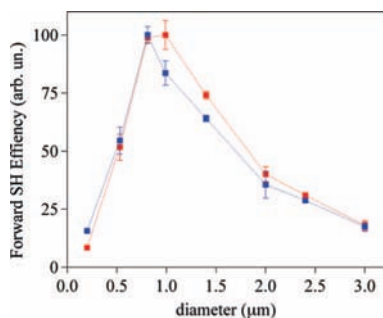


**Figure 3.** SH efficiency, in relative magnitude, measured in the forward direction for PSS particles with diameters ranging from 0.2 to 3.0  $\mu\text{m}$ . Blue and red squares represent the data with and without the multiple scattering correction, respectively. The two sets of data are normalized such that the maximum intensity corresponds to 100 units.

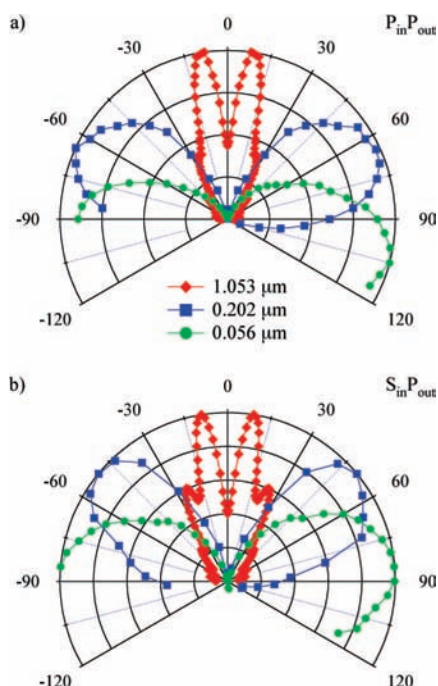


**Figure 4.** Angular distribution of SH intensity measured for PSS particles with diameters of 1.053 (red diamonds), 0.202 (blue squares), and 0.056  $\mu\text{m}$  (green circles). Two sets of polarization combinations are shown: (a) p-in/p-out and (b) s-in/p-out. Lines are used to guide the eye.

ARSHG measurements show that in the case of 0.20- $\mu\text{m}$  PSS particles, less than 10% of the SH intensity generated is detected in the forward direction. The great majority of the SH light generated from the surfaces of submicrometer- and nanometer-sized particles is in directions of large scattering angles. Previously, we have shown that by setting the detection angle at around  $90^\circ$ , which is perpendicular to the fundamental beam direction, SHG from MG adsorbed on polystyrene particles as small as 50 nm in diameter can be detected.<sup>16</sup>

It is interesting to note that the Eisenthal model based on interference between two molecules adsorbed on the opposite sides of the particle surface can be effective in estimating the angle of maximum SH intensity when the consideration is extended to include molecules on all parts of the surface. In Figure 5, the scattering angles of the maximum SH intensity for various sized particles predicted from the modified Eisenthal model (Appendix) are found to exhibit a trend such that the maximum intensity angle moves away from the forward direction as the particle diameter decreases. The modified

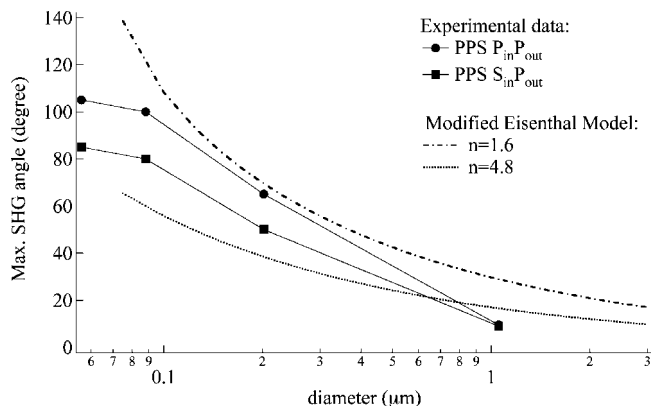


**Figure 5.** Scattering angle of the maximum SH intensity for particles with varying diameter from experimental measurements (points) and calculations using the modified Eisenthal model (lines) for two different particle refractive indices.

Eisenthal model also allows the relationships between the position of the angle of maximum intensity and the particle size for colloidal particles with large refractive indices to be examined. The case of particles with  $n_p = 4.8$  is shown in Figure 5.

The scattering angle of the maximum SHG of the large- $n_p$  particle moves toward the forward direction in comparison with the small- $n_p$  particles. This trend suggests that, as larger refractive index materials are used as colloidal particles, the maximum of SHG occurs closer to the forward scattering direction, and thus the SH intensity in the forward direction would be more likely to be detected.

#### IV. Summary and Concluding Remarks

SHG has been shown as a versatile tool for characterizing the adsorption of molecules at the surface of colloidal particles. One primary concern in applying the SHG probe is the effect of the size of the colloidal particle: in particular, for particle sizes much smaller than the optical coherent length (comparable with the light wavelengths), destructive interference of molecular polarization may render the SHG undetectable.

We have conducted measurements of SHG, using 840 nm fundamental light, from the dye molecule malachite green adsorbed on spherical polystyrene particles with various particle sizes in aqueous solutions. The measurements are performed with light polarization and scattering angle resolution. The efficiency of SHG is determined for each particle size, normalized by the density of the MG adsorbed on the particle surface, and corrected for the linear scattering of both the fundamental and SH lights by the colloidal particles in the solution. We have found that:

(1) As the SH intensity is measured in the *forward* direction (the fundamental beam propagation direction), the highest SHG efficiency occurs at  $\sim 1 \mu\text{m}$  diameter particles. SH efficiency decreases rapidly as the size decreases and becomes undetectable at diameters below 100 nm. SH efficiency also decreases when the particle size becomes larger.

(2) The SH light generated from the particle surface scatters in all directions with the angle of the maximum SH intensity tilting away from the forward direction as the particle size decreases. The angle of maximum intensity is nearly  $90^\circ$  away from the forward direction for particles with diameter smaller than 100 nm. Subsequently, in order to measure the adsorption isotherm for nanometer-sized particles the SH intensity should be detected at directions perpendicular to the fundamental beam direction.

The essence of the experimental observations can be accounted for by a straightforward phenomenological model originally proposed by Eisenthal and co-workers<sup>8</sup> based on interference between molecules adsorbed on opposite sides of the particle and is generalized for estimating SH intensity at large scattering angles. This model shows that, as the particle diameter decreases, the angle of maximum SH intensity tilts away from the forward direction. It also shows that, for a particle with larger refractive index, the SH peak shifts back toward the forward direction.

The experimental observations, particularly those associated with the smaller particles, can mostly be quantitatively accounted for using the nonlinear Rayleigh–Gans–Debye (NLRGD) model. Part II of this report will show that the NLRGD model, in the case of MG on polystyrene in water, accurately describes the particle size dependence of SHG in the forward direction for particles with diameters below 1  $\mu\text{m}$ . The NLRGD model not only generates angular distribution patterns of the scattered SH intensity in agreement with those measured for particles with diameters below 200 nm but also shows that the angle of maximum SH intensity moves toward larger angles as the particles become smaller. However, we will also show that its range of applicability is limited, and for metallic particles a more general theory, such as the Mie theory, is required.<sup>24–27</sup>

The size dependence of SH scattering angles implies that SHG can be used for applications in particle size-dependent measurements. For example, for a sample containing two varied particle sizes in the range from nano- to micrometer, the SH response can be divided into two collection geometries. The molecules adsorbed on the surface of the nanometer-sized particles can be probed at larger scattering angles. For the micrometer-sized particles, detection in the forward direction can be used to measure the SH signal from their surfaces.

**Acknowledgment.** This work is supported by a National Science Foundation GOALI Grant #0616836.

## Appendix

### A Phenomenological Model for Predicting the Scattering Angle of the SH Intensity Generated from the Surface of a Spherical Particle.

In ref 10 Eisenthal and co-workers presented a model in which only the second harmonic field, generated by nonlinear polarizations of molecules adsorbed at opposite ends of the particle, propagating along the fundamental direction is considered. In general, when considering angle-resolved SHG, the propagation directions of the fundamental and SH lights are no longer parallel to each other. Instead, there is an angle  $\theta_s$  between the two beams. The total second harmonic field from the two oppositely oriented molecules at the detector is of the form:

$$E_{2\omega} \approx \langle \beta^{(2)} \rangle E_{\omega} E_{\omega} (1 - e^{i\vec{q} \cdot \vec{d}}) \quad (\text{A1})$$

where  
with its magnitude defined as

$$\vec{q} = 2\vec{k}_{\omega} - \vec{k}_{2\omega}$$

$$|\vec{q}| = 2|\vec{k}_{2\omega}| \sin \frac{\theta_s}{2} = \frac{4\pi n_{2\omega}}{\lambda_{2\omega}} \sin \frac{\theta_s}{2}$$

The condition for constructive interference (phase matching) is

$$\vec{q} \cdot \vec{d} = \frac{4\pi n_{2\omega}}{\lambda_{2\omega}} d \sin^2 \frac{\theta_s}{2} = \pi \quad (\text{A2})$$

Equation A2 shows that phase-matched SH intensity appears at larger scattering angles with decreasing particles sizes.

## References and Notes

- (1) Antonietti, M. *Colloid Chemistry*; Springer: New York, 2003.
- (2) Evans, D. F.; Wennerstron, H. *The Colloidal Domain: Where Physics, Chemistry, Biology, and Technology Meet*, 2nd ed.; Wiley-VCH: New York, 1999.
- (3) Wang, H.; Borguet, E.; Yan, E. C. Y.; Zhang, D.; Gutow, J.; Eisenthal, K. B. *Langmuir* **1998**, *14*, 1472–1477.
- (4) Wang, H. F.; Troxler, T.; Yeh, A. G.; Dai, H. L. *Langmuir* **2000**, *16*, 2475–2481.
- (5) Eckenrode, H. M.; Dai, H. L. *Langmuir* **2004**, *20*, 9202–9209.
- (6) Subir, M.; Liu, J.; Eisenthal, K. B. *J. Phys. Chem. C* **2008**, *112*, 15809–15812.
- (7) Wang, H. F.; Yan, E. C. Y.; Liu, Y.; Eisenthal, K. B. *J. Phys. Chem. B* **1998**, *102*, 4446–4450.
- (8) Eckenrode, H. M.; Jen, S. H.; Han, J.; Yeh, A. G.; Dai, H. L. *J. Phys. Chem. B* **2005**, *109*, 4646–4653.
- (9) Yang, N.; Angerer, W. E.; Yodh, A. G. *Phys. Rev. Lett.* **2001**, *87*, 103902.
- (10) Wang, H.; Yan, E. C. Y.; Borguet, E.; Eisenthal, K. B. *Chem. Phys. Lett.* **1996**, *259*, 15–20.
- (11) Shan, J.; Dadap, J. I.; Stioipkin, I.; Reider, G. A.; Heinz, T. F. *Phys. Rev. A* **2006**, *73*, 023819.
- (12) Yan, E. C. Y.; Eisenthal, K. B. *J. Phys. Chem. B* **1999**, *103*, 6056–6060.
- (13) Liu, Y.; Dadap, J. I.; Zimdars, D.; Eisenthal, K. B. *J. Phys. Chem. B* **1999**, *103*, 2480–2486.
- (14) Srivastava, A.; Eisenthal, K. B. *Chem. Phys. Lett.* **1998**, *292*, 345–351.
- (15) Liu, J.; Subir, M.; Nguyen, K.; Eisenthal, K. B. *J. Phys. Chem. B* **2008**, *112*, 15263–15266.
- (16) Jen, S. H.; Dai, H. L. *J. Phys. Chem. B* **2006**, *110*, 23000–23003.
- (17) Weeraman, C.; Yatawara, A. K.; Bordenyuk, A. N.; Benderskii, A. V. *J. Am. Chem. Soc.* **2006**, *128*, 14244–14245.
- (18) Shen, Y. R. *The Principles of Nonlinear Optics*; Wiley: New York, 1984.
- (19) Heinz, T. F.; Chen, C. K.; Ricard, D.; Shen, Y. R. *Phys. Rev. Lett.* **1982**, *48*, 478–481.
- (20) Heinz, T. F.; Tom, H. W. K.; Shen, Y. R. *Phys. Rev. A* **1983**, *28*, 1883–1885.
- (21) Bohren, C. F.; Huffman, D. R. *Absorption and Scattering of Light by Small Particles*; Wiley: New York, 1983.
- (22) Kerker, M. *The Scattering of Light and Other Electromagnetic Radiation*; Academic: New York, 1969.
- (23) Gumprecht, R. O.; Sliepcevich, C. M. *J. Phys. Chem.* **1953**, *57*, 90–95.
- (24) Dadap, J. I.; Shan, J.; Heinz, T. F. *J. Opt. Soc. Am. B* **2004**, *21*, 1328–1347.
- (25) Pavlyukh, Y.; Hubner, W. *Phys. Rev. B* **2004**, *70*, 245434.
- (26) Hao, E. C.; Schatz, G. C.; Johnson, R. C.; Hupp, J. T. *J. Chem. Phys.* **2002**, *117*, 5963–5966.
- (27) Dadap, J. I.; Shan, J.; Eisenthal, K. B.; Heinz, T. F. *Phys. Rev. Lett.* **1999**, *83*, 4045–4048.